International Journal of Engineering, Mathematical and Physical Sciences
ISSN: 2517-9934
Vol:5, No:11, 2011

Internal Surface Measurement of Nanoparticle with Polarization-interferometric Nonlinear Confocal Microscope

Chikara Egami and Kazuhiro Kuwahara

***Abstract*—**Polarization-interferometric nonlinear confocal microscopy is proposed for measuring a nano-sized particle with optical anisotropy. The anisotropy in the particle was spectroscopically imaged through a three-dimensional distribution of third-order nonlinear dielectric polarization photoinduced.

***Keywords*—**nanoparticle, optical storage, microscope

I. Introduction

OVER time, we have been developing a tiny particles-enhanced optical data storage system using a high-resolution microscope [1], [2]. A storage medium by placing an array of tiny particles doped with dyes onto a surface relief grating was used in our system. Using reflection-type confocal optical microscopy, we measured a readout scattering signal that provides optical information recorded in tiny particles. It will be possible to increase the density of the data storage system by reducing the size of minute particles for data pits and improving the spatial resolution of the confocal microscope. The spatial resolution of the optical microscope is a critical factor for three-dimensional data storage system.

Futhermore, nanoparticles have attracted tremendous attention because of their chemical properties, which can be exploited in many optical and medical applications [3], [4]. Particlular attention, in our laboratory, has been devoted to an application of nanoparticle technology to drug delivery system (DDS) [5], [6]. Important thing to note is that the size and chemical properties on internal surface of a single particle are key factors for DDS use. With a measurement of particles less than a half wavelength of incident wave, however, general microscopes have poor spatial resolving power. This is because, in the Rayleigh scattering region, the particle exhibits the same homogeneous scattering pattern regardless of its size.

Here, in both cases the confocal microscope now in use is expected to be extremely hard to resolve spectroscopically a much smaller particle pit under the diffraction limit as well as image the three-dimensional optical anisotropy photoinduced in the single nanoparticle.

C. Egami is with Faculty of Engineering, Shizuoka University, 3-5-1 Johoku Naka-ku Hamamatsu Shizuoka, 432-8561, Japan (phone: +81-53-478-111; fax: +81-53-478-1113; e-mail: tdcegam@ipc.shizuoka.ac.jp).

K. Kuwahara is with Faculty of Engineering, Shizuoka University, 3-5-1 Johoku Naka-ku Hamamatsu, Shizuoka, 432-8561, Japan (phone: +81-53-478-1612; e-mail: tekkuwa@ipc.shizuoka.ac.jp)

In this paper, incorporating a polarization interferometer into a nonlinear confocal microscope, we propose polarization-interferometric nonlinear confocal microscopy in order to observe nano-sized objects with inhomogeneous linear absorption. We can observe a three-dimensional distribution of third-order optical nonlinearity ($P^{(3)}$) which incoming coherent light induces in the objects.

An organic chromophore-doped particle (200 to 300-nm diameter) in a rigid polymer matrix was employed as a sample of the nano-sized objects. The particle with linear absorption acts as nonlinear optical materials for high-intense cw laser illumination. A laser diode (LD) with an emission wavelength of λ =635 nm in the wing of its absorption spectrum was used.

A laser beam focused by a high-NA objective lens onto the particle generates the nonlinear dielectric polarization, which provides backscattering from it. Polarization analysis of the scattered signal by means of polarization interferometry observes the $\chi^{(3)}$ distribution in the particle. Also, phase analysis of the scattered signal by means of Michelson interferometry estimates a change in the refractive index of the particle.

We have succeeded in measuring not only the optical shape of the single nano particle but also microscopic photo-anisotropic distribution induced in it.

II. Theoretical Model

In homogeneous objects with weak linear absorption, coherent light stimulates the third-order nonlinear polarization depending on its intensity and polarization state. The mutual interaction of incident beams generates the nonlinear polarization with specific susceptibility tensor elements. In general, homogeneous objects, which exhibit the third-order optical nonlinearity, have nonzero tensor elements of $\chi^{(3)}_{ijkl}$. Each element is denoted by its Cartesian indices. There are 21 nonzero elements, of which only 3 are independent. They are

$$\begin{aligned} &yyzz = zzyy = zzxx = xxzz = xxyy = yyxx,\\ &yzyz = zyzy = zxzx = xzxz = xyxy = yxyx,\\ &yzzy = zyyz = zxxz = xzzx = xyyx = yxxy, \end{aligned} \quad (1)$$

also

$$xxxx = yyyy = zzzz = xxyy + xyxy + xyyx.$$

Here, incident and outgoing beams are assumed to be inclined to each other at an angle small enough to allow us to neglect the influence of the z components of the fields

concerned. The nonlinear susceptibility of homogeneous objects has non-vanishing components:

$$\chi^{(3)}_{xxyy}(-\varpi,\varpi,\varpi,-\varpi)=\chi^{(3)}_{yyxx}(-\varpi,\varpi,\varpi,-\varpi),$$
$$\chi^{(3)}_{xyxy}(-\varpi,\varpi,\varpi,-\varpi)=\chi^{(3)}_{yxyx}(-\varpi,\varpi,\varpi,-\varpi),$$
$$\chi^{(3)}_{xyyx}(-\varpi,\varpi,\varpi,-\varpi)=\chi^{(3)}_{yxxy}(-\varpi,\varpi,\varpi,-\varpi),$$

also (2)

$$\chi^{(3)}_{xxxx}(-\varpi,\varpi,\varpi,-\varpi)=\chi^{(3)}_{yyyy}(-\varpi,\varpi,\varpi,-\varpi)$$
$$=\chi^{(3)}_{xxyy}(-\varpi,\varpi,\varpi,-\varpi)+\chi^{(3)}_{xyxy}(-\varpi,\varpi,\varpi,-\varpi)+\chi^{(3)}_{xyyx}(-\varpi,\varpi,\varpi,-\varpi).$$

In the objects, also, the above relation is in balance. We should note, in passing, that the relation, in inhomogeneous objects, becomes out of balance; $\chi^{(3)}_{xxxx}(-\varpi,\varpi,\varpi,-\varpi)$ loses and vanishes consequently. Let us return to homogeneous objects; the nonlinear polarization are represented as

$$P^{(3)}=\varepsilon_0\chi^{(3)}:EEE \tag{3}$$

where ε_0 is the dielectric constant in vacuum. The field amplitude vector E at frequency ϖ sums up that of the incident and outgoing beams. The nonlinear polarization as a field source induces scattering. The scattered light (E_s) is given by

$$E_S \propto \left|\ddot{P}^{(3)}\right|. \tag{4}$$

The confocal optical microscope detects conventional linear scattering as well as the intensity-enhanced nonlinear scattering near a focal point. When the incident beam has a linearly x-polarized field amplitude vector, $\chi^{(3)}$ is expressed as $\chi^{(3)}_{xxxx}(-\varpi,\varpi,\varpi,-\varpi)$ composed of the three independent components.

Suppose a small absorptive semi-homogeneous object, or a partially chromophore-doped nanoparticle, is in a large transparent homogeneous matrix, or a polymer/liquid matrix. For low-intensity-beam confocal imaging, on the one hand, both the object and the matrix scatter coplanar light. For high-intensity-beam confocal imaging of it, on the other hand, the object scatters anisotropic noncoplanar light and the matrix scatters coplanar light. Negligible optical nonlinearity generates in the semi-homogeneous object while no nonlinearity generates in the homogeneous matrix due to transparency of itself; the intensity-enhanced nonlinear scattering from the semi-homogeneous one occurs near a focal point. It is well known in organic dye molecules like saturable absorbers that an intense incident beam generates a transition dipole moment in an excited state being oriented at an angle to that in a ground state; the resultant nonlinear polarization scatters feeble nonisotropic light according to its molecular structure [7]. This is equivalent to induction of any out of three susceptibility components composing $\chi^{(3)}_{xxxx}(-\varpi,\varpi,\varpi,-\varpi)$ in the semi-homegeneous objects. General intense-beam confocal imaging observes not only the semi-homogeneous object but also the homogeneous background matrix, because the object signal to the matrix signal ratio is very low. Of particular interest is the special case when the partially inhomogeneous object, or semi-homogeneous one, is illuminated with an intense laser beam, which induces any out of three

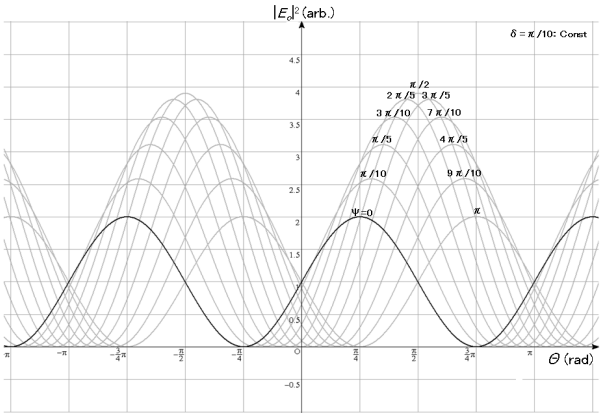

Fig. 1 Analyzer-angle dependence of the scattered irradiance with changing ϕ

susceptibility components composing $\chi^{(3)}_{xxxx}(-\varpi,\varpi,\varpi,-\varpi)$ even in the inhomegeneous objects. A resulting y-vector component yields only if the object possesses nonlinear optical anisotropy due to the anti-symmetric tensor properties of objects. The confocal microscope with a polarization interferometer emphasizes the y-vector component while reducing the x-component scattering from the homogeneous background. As a result, the internal surface photoanisotropy induced in the nanoparticle can be measured while enhancing any of the three components constituting $\chi^{(3)}_{xxxx}(-\varpi,\varpi,\varpi,-\varpi)$.

Here, with a polarization interferometer suppressing the isotropic light scattering from the homogeneous matrix, the background matrix image goes black; the $\chi^{(3)}$-induced object image stands out in bold relief against it. The homogeneous matrix background image goes black. General confocal imaging observes only the boundary between the object and the matrix due to too low scattering signal from the semi-homogeneous objects.

Suppose now that two coherent beams of light interfere on a photodetector. In accordance with the principle of superposition, an interferometric electric field vector E_o, at a point on the photodetector, is given by

$$E_o = E_S + E_R \tag{5}$$

where E_s is the elliptically polarized field vector of the scattered light and E_R is the y-polarized field vector of a reference beam, both of which are traveling in the z-direction. Written in Johnes matrix column form, the two fields are

$$E_S = A_S\begin{pmatrix}\cos\psi\\ \sin\psi e^{i\delta}\end{pmatrix} \tag{6}$$

and

$$E_R = A_R\begin{pmatrix}0\\1\end{pmatrix}. \tag{7}$$

Here A_s and A_R are the field amplitudes of the two vectors, respectively, ϕ is the angle between principal axes of ellipse and the (x, y)-coordinate axes, and δ is the phase difference between the x and y components of E_s. In a general confocal

microscopy, which has no sensitivity to photoanisotropy, scattered light irradiance is independent of changes not only in δ but also in ϕ, namely,

$$\left(\frac{\partial|E_S|^2}{\partial\delta}\right)_{\psi}=0, \tag{8}$$

$$\left(\frac{\partial|E_S|^2}{\partial\psi}\right)_{\delta}=0. \tag{9}$$

The microscope, which is unable to respond to dichroism and birefringence, the resulting confocal images reduce a contrast-transfer function (CTF). Suppose then that we introduce an analyzer in front of the detector, whose transmission axis makes a counterclockwise angle θ to be positive with the coordinate system. Here if θ =0, the Johnes matrix formalism of the analyzer is given by

$$[M(\theta=0)]=\begin{bmatrix}1 & 0\\ 0 & 0\end{bmatrix}. \tag{10}$$

Also, since a counterclockwise rotation in the xy-plane by the rotation angle θ brings about the following transformation matrix

$$[T(\theta)]=\begin{bmatrix}\cos\theta & \sin\theta\\ -\sin\theta & \cos\theta\end{bmatrix}, \tag{11}$$

the rotated Johnes matrix for the analyzer has the mathematical form

$$\begin{aligned}[M(\theta)]&=[T(-\theta)][M(\theta=0)][T(+\theta)]\\ &=\begin{bmatrix}\cos^2\theta & \sin\theta\cos\theta\\ \sin\theta\cos\theta & \sin^2\theta\end{bmatrix}.\end{aligned} \tag{12}$$

As a result, the interferometric electric field vector through the analyzer is given by

$$\begin{aligned}E_o&=[M(\theta)](E_s+E_R)\\ &=\begin{pmatrix}A_S\cos^2\theta\cos\psi+\sin\theta\cos\theta\left(A_S\sin\psi e^{i\delta}+A_R\right)\\ A_S\sin\theta\cos\theta\cos\psi+\sin^2\theta\left(A_S\sin\psi e^{i\delta}+A_R\right)\end{pmatrix}=\begin{pmatrix}E_x\\ E_y\end{pmatrix}.\end{aligned} \tag{13}$$

Suppose now that $A_s \simeq A_R$, the angle dependent irradiance can be rewritten as

$$\begin{aligned}|E_o|^2&=|A_S|^2[\cos^4\theta\cos^2\psi+\frac{1}{4}\sin^2 2\theta\\ &+\left(\frac{1}{4}\sin^2 2\theta+\sin^4\theta\right)\left(1+\sin^2\psi+2\sin\psi\cos\delta\right)\\ &+\sin 2\theta\cos\psi\left(1+\sin\psi\cos\delta\right)].\end{aligned} \tag{14}$$

To examine the effect of the polarization interferometry, we have computed the results shown in Fig. 1 calculated from (14) using $\delta=\pi/10$. If we let $\phi=0$ then the maximum and minimum irradiances, for example, occur when $\theta=+\pi/4\pm n\pi$ and $-\pi/4\pm n\pi$ (n=0.1.2…). We note that the irradiances correspond to positive and negative images for the polarization interferometric observation, respectively. When a x-polarized beam strikes a transparent homogeneous matrix then the orientation of the electric field of the scattered signal E_s follows the dipole pattern induced, which is parallel to the electric field of the incoming beam, that is, ϕ =0 in (13). We obtain

$$E_o(\psi=0)=\begin{pmatrix}A_S\cos^2\theta+A_R\sin\theta\cos\theta\\ A_S\sin\theta\cos\theta+A_R\sin^2\theta\end{pmatrix}. \tag{15}$$

Notice that the signal does not depend on the phase difference δ. This just means that, even if the matrix is homogeneous, the scattered signal is independent from the refractive index distribution. Suppose now that $A_s \simeq A_R$, the angle dependent irradiance can be rewritten as

$$\approx A_S\begin{pmatrix}\cos^2\theta-\sin\theta\cos\theta\\ -\sin\theta\cos\theta+\sin^2\theta\end{pmatrix}. \tag{16}$$

In order to suppress scattering from the homogeneous background matrix, we adjust the x and y components of the field being equal at $\theta=-\pi/4$. What we should note is that the procedure is equivalent to operating the vector subtraction of the signal and reference beams, or making the background signal equal to zero. As a result, the operation, in which the CTF approaches maximum value, enhances the contrast resolution of the confocal imaging. We now consider the case where an intense x-polarized beam scans a semi-homogeneous small object surrounded by the homogeneous background matrix. The scattered light irradiance through the analyzer with its transmission axis at $\theta=-\pi/4$ is, according to (13), given by

$$\begin{aligned}\left|E_o\left(\theta=-\pi/4\right)\right|^2&=\left|E_x\left(\theta=-\pi/4\right)\right|^2+\left|E_y\left(\theta=-\pi/4\right)\right|^2\\ &=|A_S|^2\left(1-\cos\psi+\sin\psi\cos\delta-\frac{1}{2}\sin 2\psi\cos\delta\right).\end{aligned} \tag{17}$$

The result equivalently expresses the electric-field-vector subtraction between the scattered light and the reference beam by means of the polarization interferometer. Consequently, the equation means significant polarization-interferometric irradiance change with ϕ even in the case of objects with δ =0. Respond to the change in ϕ. Also, taking appropriate partial derivatives of the above irradiance with respect to ϕ and δ, holding δ and ϕ constant, we get and as such is plotted in Fig.2.

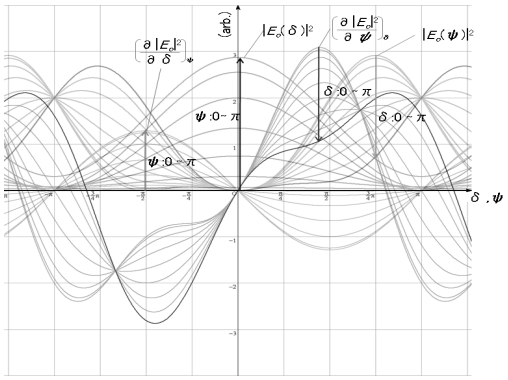

Fig. 2 Optical response for a polarization-interferometric irradiance change with δ and ϕ

$$\left(\frac{\partial\left|E_o(\theta=-\pi/4)\right|^2}{\partial\psi}\right)_{\delta}=\frac{\left|A_S\right|^2}{2}\left[(\cos\psi-\cos 2\psi)\cos\delta+2\sin\psi\right], \quad (18)$$

$$\left(\frac{\partial\left|E_o(\theta=-\pi/4)\right|^2}{\partial\delta}\right)_{\psi}=\left|A_S\right|^2\left[\left(-\sin\psi+\frac{1}{2}\sin 2\psi\right)\sin\delta\right], \quad (19)$$

On the one hand, for $-\pi/4<\phi<\pi/4$, the irradiance $|E_o(\psi)|^2$ is very low and flat. On the other hand, the irradiance $|E_o(\delta)|^2$ is very high and its change in ϕ with respect to δ is very steep. What we should stress is that, semi-homogeneous objects, in general, have only smaller δ compared with small ϕ. The polarization-interferometric system with the electric-field vector subtraction operation can detect objects with slightly tilted optical axis, or a light declination from homogeneous $\chi^{(3)}_{xxxx}(-\varpi,\varpi,\varpi,-\varpi)$. The optical tilting angle ϕ plays a key role in the photoanisotropic scattering in comparison to the phase change in δ.

As a last example, the scattered light irradiance through the analyzer with its transmission axis at $\theta=+\pi/4$ is, according to (11), given by

$$\left|E_{out}\left(\theta=+\pi/4\right)\right|^2=\left|E_x\left(\theta=+\pi/4\right)\right|^2+\left|E_y\left(\theta=+\pi/4\right)\right|^2$$
$$=\left|A_S\right|^2\left(1+\cos\psi+\sin\psi\cos\delta+\frac{1}{2}\sin 2\psi\cos\delta\right). \quad (20)$$

The result equivalently expresses the electric-field-vector addition between the scattered light and the reference beam by means of the polarization interferometer.

III. Experimental Setup

A schematic of a polarization-interferometric nonlinear confocal microscopy is shown in Fig. 3. A core optical configuration including the Michelson interferometer for polarization interferometry is a confocal microscope. A laser diode (LD) with an emission wavelength of λ = 635 nm is used. A LD's output beam as being s-polarized travels through a beam expander to optimize the numerical aperture (NA) of objective lenses, which determines the basic resolving power of the confocal microscope.The beam divides into a reference-arm beam and a measurement-arm beam. The reference-arm and measurement-arm beams are focused onto a mirror and a sample, respectively, by two identical microscope objective lenses with a NA of 0.9. We measured the axial resolution of the conventional confocal microscope by using a mirror as a sample. The Full Width, at Half Maximum (FWHM), is defined as the microscope's resolution. The basic confocal microscope has an axial resolution of 0.7 μm, which is limited by its NA.

The reference-arm beam also provides conventional intensity-type interference by introducing reflected light, using a standard configuration of a quarter-wave plate (λ/4) and the polarizing beam splitter (BS1). On the measurement arm, on the other hand, a sample is mounted on 5-nm-resolution three-axis piezo stages. The measurement beam focused onto the sample induces a nonlinear dielectric polarization, which provides backscattering from it. Analysis of the scattered signal estimates the dielectric polarization on the construction of the sample. After passing through an optional pinhole of diameter

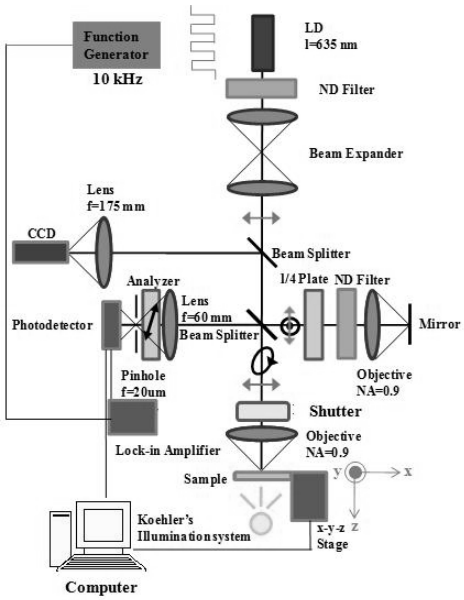

Fig. 3 Optical setup for a polarization-interferometric nonlinear confocal microscopy

20 μm, the interferometer's output intensities into a lock-in amplifier are measured. The current modulated LD for improving the signal-to-noise ratio in the interferometer is employed to generate a chopping frequency of 10 kHz for the lock-in reference.

A principle of polarization-vector interferometry in the nonlinear confocal microsope is summarized below. The high-intensity focused beam as being linearly polarized induces the nonlinear dielectric polarization ($P^{(3)}$) in a sample medium. When the dielectric polarization occurs, light is backscattered while traveling through the medium. Assume that an optical axis of the medium has an orientation that is oblique, but not perpendicular or parallel to the polarization-vector orientation of the focused beam. In this case, the backscattered light has any elliptical polarization state, which is dependent on localized third-order optical nonlinearity ($P^{(3)}$) of the medium. In other words, the polarization state of the backscattered light is composed of s- and p- polarization components with some phase difference. The amplitude of the polarization components and the phase difference between them are determined by $P^{(3)}$ due to medium's properties.

The confocal microscope equips itself with a thin film analyzer to allow for polarization-vector interference between the two components. Rotating the analyzer's transmission axis by some degrees with respect to that of the focused beam's polarization modulates the amplitude of a light wave passing through the analyzer. The analyzer is utilized to control the amount of light waves passing through itself, and can be rotated in the light path to enable various amplitudes of polarized light to pass through.

The analyzer is initially positioned with its transmission axis parallel to a polarization-vector orientation (θ = 0) of the focused beam. In this case, the microscope functions as the

conventional confocal one. In addition, when the focused beam's polarization and analyzer are completely crossed ($\theta = \pi/2$), the vertical component becomes negligible and the polarizers have achieved their maximum extinction value.

There are also two typical ways to use the polarization interferometer: on the one hand, when the analyzer axis is set at near $\theta = \pi/4$, the microscope functions as the positive-type one to add the signals of s- and p-components; but, on the other hand, when the analyzer axis is set at near $\theta = -\pi/4$, the microscope functions as the subtraction-type one to calculate the difference signals between the two components. The analyzer angle depends on not only the scattered light's intensity but also the microscopic optical axis direction of the sample. Here, in the subtraction-type microscope, we set the confocal signal minimum while scanning the background outside of objects. The polarization-interferometric confocal signal from the background becomes negligible when it has a homogeneous sample background; the contrast of the image becomes large when the medium has an inhomogeneous sample object. This results in a bright sample image on a darker background. The objects areas with $P^{(3)}$ can be observed in the microscope and shine out against the dark background with high contrast.

IV. Results And Discussion

A polymer matrix dispersed with organic-dye-doped polystyrene particles (ϕ = 200 nm) was prepared as a sample object. The polymer matrix macroscopically has an optical density of 0.1 at 635 nm. Therefore, the absorptive matrix exhibits very low scattering. As a result, it is difficult to resolve the conventional confocal signal of a single particle.We observed the subtraction signal between the polarization vector of the reference beam and that of the scattered light due to the $P^{(3)}$ by using the nonlinear confocal microscope. The microscope, in this case, functions as the subtraction-type one so as to suppress the background signal around the top of the particle. We pre-measured the approximate depth level of the particles with the conventional confocal microscope. After that, we laterally scanned the nano particles with the nonlinear microscope while focusing on tops of ones in a coplanar. Scan area is 1μm x 1μm. Firstly, the solid-line squared images in Fig. 4 (a), which is correspond to subtractive operation at $\theta = -2/9\pi$ near $-\pi/4$, expresses the top of two particles in a plane. With a decrease of the scattered signal in the peripheral portions of the particle, the image's contrast resolution is emphasized on the top of the particles. The resolution measured about 12 nm. The experiment with the negative type confocal microscope proved that the CTF was enhanced by measuring the difference signal while depressing the background signal. Secondly, the dashed-line squared image in Fig. 4 (b) expresses the top of a single particle in another plane. The axial position of the particle is different from that of the particles surrounded by the solid line. For that reason, the angle of the analyzer deviated from $-2/9\,\pi$. In other words, the experiment proved that the polarization-interferometric confocal microscope can image serial z-axis optical sections by rotating the analyzer instead of scanning the sample in the axial direction.

Firstly, the particle's diameter measured about 200 nm with the addition-type confocal microscope. The value by the

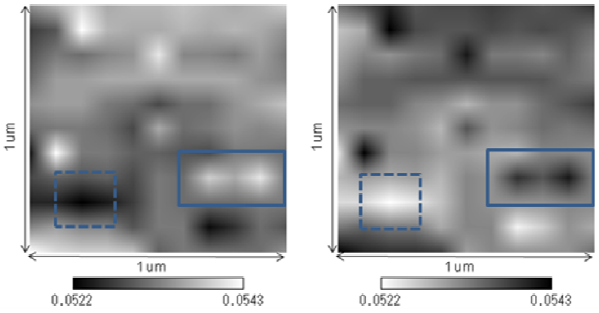

Fig. 4 Profiles of the polarization- interferometric cofocal images of the nano particles in different axial positions: the analyzer transmission axis (a) at $\theta = -2/9\pi$ and (b) at $\theta = -5/18\pi$. (scan area, 1μm x 1μm).

method well agreed with that by electron microscopy. Secondly, the internal surface of the single particle was measured with the subtraction-type optical system proposed. Fig. 5 shows individual tomographic images of the single nano particle with the polarization-interferometric nonlinear confocal microscope, showing that different sections visualize the $\chi^{(3)}$ distribution at z = 30, 40, 50, 60 nm (as examples of typical images). The microscope functions as the subtraction-type one. Scan area, is 100 nm x 100 nm. Successive serial optical sections were recorded along the z optical axis of the microscope. The microscopic inhomogeneous $\chi^{(3)}$ distribution was measured even in absorptive nano-sized object. Introducing the polarization-vector interferometry enhanced the spatial resolution of the confocal system both in axial and lateral directions.

The subtraction-type confocal microscope have realized the contrast resolution, or CTF, enhancement by measuring the $\chi^{(3)}$ distribution showing the microscopic refractive index change in the particle. The system is proven to be effective for imaging nano-sized absorptive objects with low scattering.

V. Conclusion

Incorporating a polarization interferometer into a nonlinear confocal microscope, we propose polarization-interferometric nonlinear confocal microscopy in order to observe nano-sized objects with inhomogeneous linear absorption. We have succeeded in observing a three-dimensional distribution of the optical anisotropy in the organic chromophore-doped particle (200-nm diameter) in the rigid polymer matrix which incoming coherent light induces in it.

Acknowledgment

This work has been supported in part by a grant in aid for fundamental scientific research from the Ministry of Education, Culture, Sports, Science and Technology of Japan.

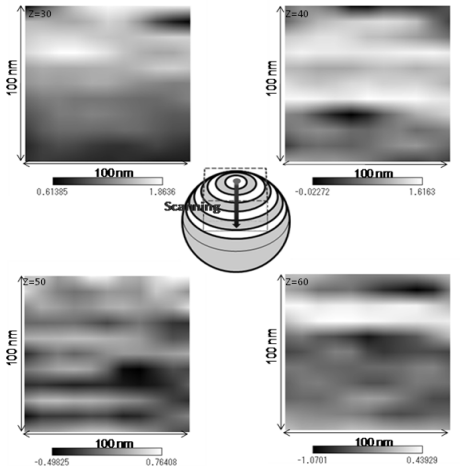

Fig. 5 Individual confocal images of a single particle, shwing that different sections visualize the $P^{(3)}$ distribution at z = 30, 40, 50, 60 nm. (scan area, 100nm x 100nm). The analyzer transmission axis is set at $\theta = -2/9\pi$. Successive serial optical sections were recorded along the z optical axis of the microscope

REFERENCES

[1] N. Kobayashi and C. Egami, "High-resolution optical storage by use of minute spheres", Opt. Lett. **30**, 2005, pp. 299-301.
[2] C. Egami, N. Nishimura, and T. Okawa, "Jitter-free multi-layered nanoparticles optical storage disk with buffer ring ", Opt. Exp. Vol. 18, Iss. 15, 2010, pp. 15901-15906.
[3] W. Weise, P. Zinin, T. Wilson, A. Briggs, S. Boseck, "Imaging of spheres with the confocal scanning optical microscope", Opt. Lett. **21**, 1996, pp. 1800-1802.
[4] C. E. Bigelow, D. L. Conover, and T. H. Foster, "Confocal fluorescence spectroscopy and anisotropy imaging system", Opt. Lett. **28**, 2003, pp. 695-697.
[5] W. H. D. Jong and P. J. Borm, "Drug delivery and nanoparticles: applications and hazards", Int. J. Nanomedic. Vol. **3** (2), 2008, pp. 133-149.
[6] D. A. Canelas, K. P. Herlihy, and J. M. DeSimone, "Top-down particle fabrication: control of size and shape for diagnostic imaging and drug delivery", Wiley Interdiscip Rev. Nanomed. Nanobiotechnol. 2009 Vol. 1(4), pp.391-404.
[7] T. Sato and S. Miyanaga, "Polarization-dependent phase-conjugate reflectivity in randomly oriented saturable absorbers: effects of direction of transition dipole moment associated with excited-state absorption", Opt. Rev. , Vol. 6, 1999, pp. 522-528.